ORIGINAL ARTICLE

Re-evaluation of the centrifuge method for describing the unsaturated hydraulic functions of porous rock and till soil samples

Maria C. Caputo[1] | Lorenzo De Carlo[1] | Antonietta C. Turturro[1] | Horst H. Gerke[2]

[1]CNR National Research Council, IRSA Water Research Institute, Bari, Italy

[2]Research Area 1 "Landscape Functioning", Leibniz-Centre for Agricultural Landscape Research (ZALF), Müncheberg, Germany

Correspondence
Maria C. Caputo, CNR National Research Council, IRSA Water Research Institute, via Francesco De Blasio 5, Bari 70132, Italy.
Email: mariaclementina.caputo@cnr.it

Assigned to Associate Editor Giuseppe Brunetti.

Abstract

The determination of hydraulic characteristics as a function of the pressure head is laborious and data ranges are restricted. Indirect methods to estimate $K(h)$ are introducing additional uncertainty and the method-dependent restricted data ranges that can hamper a bimodal curve fitting. The objective of this study was to re-evaluate the centrifuge approach for directly measuring the unsaturated hydraulic properties of porous carbonate rock and glacial till soil samples. Hydraulic conductivity was determined by means of evaporation (EVA), quasi-steady centrifuge (QSC), and double-membrane steady-through flow (DMSTF) methods. Retention curves were obtained by using the EVA, QSC, mercury intrusion porosimetry (MIP), suction table, and pressure chamber. The tested samples belong to two rock lithotypes coming from the Apulia region, southern Italy, and three soil clods of dense glacial till parent material collected in northeastern Germany. Unimodal and bimodal hydraulic functions were used to fit hydraulic conductivity and retention data. The QSC data of the highly dense soil clods qualitatively demonstrated the different effects of bulk density and rigidity on the soil hydraulic functions. The MIP data showed the existence of a bimodal pore size distribution. The combination of data obtained by EVA, QSC, and DMSTF methods improved the fitting of the bimodal hydraulic conductivity functions to data of both rock and soil samples. The results confirm the uniqueness of the QSC method for measuring the hydraulic conductivity in a wider range of matric potential value and its limitation for nonrigid samples even if they are of high density.

Plain Language Summary

The vadose zone, the region between the soil surface and the water table, is important in affecting groundwater quality and quantity, ecosystem, human health, and

---

Abbreviations: DMSTF, double-membrane steady-through flow; EVA, evaporation; MIP, mercury intrusion porosimetry; MRC, mercury retention curve; PC, pressure chambers; PDI, Peters Durner Iden; QSC, quasi-steady centrifuge; ST, suction table; vG, van Genuchten; WRC, water retention curve.

natural risks. Essential phenomena take place in the vadose zone, as water and pollutants are transported and stored in the subsoil, and interactions among air, water, soil, rocks, contaminants, and microorganisms occur. Knowledge of flow processes is crucial for water management and safeguarding by implying the determination of hydraulic characteristics of the media constituting the subsoil. This study compares different methods for measuring hydraulic properties that control the water flow and the contaminants transport in the vadose zone. The outcomes show that not all the methods work for soils and rocks, and some of them provide accurate data. Results provide hydraulic parameters for numerical modeling of flow and transport processes to solve environmental problems and manage the anthropic actions to prevent the risk for human health.

1 | INTRODUCTION

The unsaturated zone, that is, the region between the soil surface and the water table, plays an important hydrologic role since it affects groundwater quality and quantity, ecosystem and human health, nutrient cycle, soil development, and natural risks (Perkins, 2011). Essential hydrobio-geo-chemical phenomena take place in the unsaturated zone, such as water transport and storage into the subsoil, filtering of pollutants transported by fluids moving under variably saturated conditions, and interactions among air, water, soil, rocks, contaminants, and microorganisms (Perkins, 2011). Quantitative knowledge of unsaturated flow processes is crucial for water management and safeguard, as well as for evaluating groundwater recharge (Caputo & De Carlo, 2011).

Variably saturated flow in the unsaturated zone has frequently been described with the Richards' (1931) equation (Šimůnek et al., 2016). The equation is given in the pressure head-based one-dimensional form as:

$$C\frac{\partial h}{\partial t} = \frac{\partial}{\partial z}\left[K(h)\frac{\partial h}{\partial z} + K(h)\right] \qquad (1)$$

where h (L) is the pressure head or matric potential, K (L T^{-1}) is the hydraulic conductivity as a function of h, z (L) is the vertical coordinate, here directed positive upward, t (T) is time, and C (L^{-1}) is the water capacity, that is, $C = \mathrm{d}\theta/\mathrm{d}h$ is the slope of the water retention function, with θ (L^3 L^{-3}) the volumetric water content. The solution of the Richards' equation requires two hydraulic functions for characterizing the porous medium, which are the water retention curve (WRC) $\theta(h)$ and the hydraulic conductivity function $K(h)$; especially the latter is usually a highly nonlinear function of h (Perkins, 2011).

Despite recent progress in pedotransfer functions (Puhlmann & von Wilpert, 2012; Singh et al., 2021) and inverse optimization (Iden & Durner, 2007; Vrugt et al., 2008; Wöhling et al., 2008), the estimation of unsaturated hydraulic properties is still limited by uncertain heterogeneity of the highly complex pore structures (Durner & Lipsius,

2005). For indirectly estimating unsaturated hydraulic functions, the more easily available data, such as particle size distributions, texture, bulk density, and organic matter content, are used in hydraulic pedotransfer functions, or alternatively, a relative K function can be predicted from the WRC and combined with a measured value of the saturated hydraulic conductivity (K_s) (Durner & Lipsius, 2005). Nevertheless, direct measurements are still necessary since also the procedures for indirect K estimation need data as benchmark for validation. However, the direct measurement, especially of $K(h)$, in the field and in the laboratory, is not only laborious, costly, and time-consuming (Durner & Lipsius, 2005) but also mostly severely limited to a small range of h and θ values, depending on the method itself. Among the indirect methods, the geophysical techniques, such as electrical resistivity tomography and electromagnetic induction, have often been used to monitor unsaturated flow processes by identifying the hydraulic properties (Caputo et al., 2023; De Carlo et al., 2021, 2023; Doussan & Ruy, 2009; Farzamian et al., 2015; Masciopinto & Caputo, 2011; Zhang et al., 2023).

Durner and Lipsius (2005) described various infiltration methods carried out both in steady and unsteady conditions by installing a large infiltrometer ring, TDR probe (time-domain reflectometry), and tensiometers to monitor θ and h during the infiltration in order to determine $K(h)$ by using instantaneous profile analysis. However, these methods have rarely been used in outcropping rocks, because the θ and h monitoring at different depths, for long periods after infiltration, needs laborious installation of TDR probe, or similar probes, which are difficult to insert into the rocks. The K measurements in the laboratory have the advantage of better control of environmental and boundary conditions, and of more easy flux rate and water content measurements. Due to improved automated control and precise data acquisition with relatively high temporal resolution during the tests, laboratory methods allow accurate hydraulic conductivity measurements (Durner et al., 1999). Direct laboratory methods can be carried out

both under steady-state flux and under transient conditions to measure the values of the hydraulic conductivity at specific pore water saturations for determining the $K(h)$ function (Durner & Lipsius, 2005).

The steady-state methods are particularly suitable to determine K values near saturated conditions, but are time-consuming, tedious, and expensive. Moreover, they lose their attractiveness in dry condition because of the complexity in obtaining constant fluxes and unit gradients (Durner & Lipsius, 2005).

The crust method (Bouma et al., 1983) and the drip infiltrometer (Dirksen, 1991) are particularly laborious to obtain $K(h)$ in the whole range of h. The steady-state evaporation method (Fujimaki & Inoue, 2003) requires independent determination of $\theta(h)$. The disc infiltrometer method (Šimůnek et al., 1999) or double-membrane steady-through flow (DMSTF) (Rieckh et al., 2012) does not give estimates of K_s. The heat pipe method (Globus & Gee, 1995), which allows K measurements for very low values of h, requires temperature control and an independent determination of $\theta(h)$, which is more than being time-consuming.

Moreover, the suction table (ST) (Romano et al., 2002) as well as the pressure cell or pressure chambers (PC) (Dane & Hopmans, 2002) methods, commonly used to obtain $\theta(h)$ function, do not allow to measure the $K(h)$ function.

Unlike steady-state methods, the transient methods, such as one-step and multistep outflow (van Dam et al., 1990), evaporation (EVA) (Wind, 1968), and downward (Zou et al., 2001) and upward (Hudson et al., 1996) infiltration methods, are more rapid because they do not need equilibrium steps. However, most of these methods are not suitable to determine $K(h)$ in the wet range by showing low sensitivity to K at or near saturation conditions, except for the multistep outflow method (Zhuang et al., 2017).

Thus, Perkins (2011) suggested that the most reliable measurements of K values came from steady-state flow methods, although they were still rarely applied because of the time needed to get single K values in case of gravity-driven implementation. This limitation was coped with by applying the centrifugal force to the sample in order to establish the moisture steady-state condition and allow rapid measuring of $K(h)$ up to the very dry range. From the few studies that tested methods to measure the $K(h)$ of porous rocks, Lipovetsky et al. (2020) used the EVA and chilled-mirror dewpoint (Campbell et al., 2007) to estimate $K(h)$ of two Indiana limestone rock samples. Caputo and Nimmo (2005) used three different lithotypes of rocks to test the quasi-steady centrifuge (QSC) method; an experimental apparatus, consisting of a control flow reservoir placed above a sample and an outflow disk below the sample, was inserted in a bucket of the BECKMAN Model J-6 M centrifuge to measure unsaturated hydraulic conductivity on rock samples. In a previous paper, Turturro et al. (2020) demonstrated the direct proportionality between flux and applied centrifugal force in the centrifugal field when

Core Ideas

- Test of rapid quasi-steady centrifuge (QSC) method for nonrigid soil clods of high density versus porous rock.
- Comparison of full-range QSC with partial-range methods for determining hydraulic properties.
- Fitting of uni- and bimodal hydraulic functions to full- and combined partial-range datasets.
- Continuous QSC data near saturation support bimodal fitting of hydraulic functions.
- Application of QSC method to soil clods with high density but nonrigid pore structure.

measuring the $K(h)$ function of carbonate porous rocks. This short review shows that hardly any method exists to directly measure K values along a broader range of water content or pressure head values. In addition, studies that compare unsaturated hydraulic functions $\theta(h)$ and $K(h)$ of soils with those of rocks are limited.

Especially the measurement of the hydraulic conductivity function, $K(h)$, is laborious, and data are mostly limited to restricted method-dependent moisture ranges. Indirect methods to estimate $K(h)$ from the WRC or by pedotransfer functions are introducing additional uncertainty. Furthermore, the method-dependent restricted data ranges can hamper the identification and fitting of bimodal hydraulic functions at higher water saturations. We hypothesize that datasets obtained from QSC in combination with steady- and transient-flow methods can be useful for improving the representation of characteristic hydraulic functions. Especially for fitting bimodal functions of structured soils, the $K(h)$ function in the higher moisture range could be complemented by using the QSC method.

Four variants of hydraulic model, which are the unimodal (van Genuchten, 1980) and bimodal of both van Genuchten (vG) and Peters Durner Iden (PDI) (Caputo et al., 2022; Iden & Durner, 2014; Peters, 2014) type functions, were applied to the retention and hydraulic conductivity data, obtained by the abovementioned methods, by using the HYPROP-FIT (now LABROS SoilView Analysis v5.1.1.0) software. Covering the complete moisture range, PDI model considers the hydraulic conductivity as the sum of capillary and film conductivity. Since its formulation is quite complicated, it is referred to LABROS SoilView Analysis Manual (Pertassek et al., 2015). Bimodal formulations of vG and PDI hydraulic conductivity functions were used in order to capture the dual porosity of the tested media.

The objective of this study was to re-evaluate the centrifuge approach in comparison with other laboratory methods for directly measuring the unsaturated hydraulic properties

using data from porous carbonate rock and glacial till soil samples. The hydraulic conductivity functions of carbonate porous rocks and soil clod samples were obtained from the experimental data directly measured using the EVA, QSC, and DMSTF methods. WRCs were obtained by using the EVA, QSC, ST, and PC methods. The pore size distribution measured by mercury intrusion porosimetry (MIP) was used to verify if the assumption of fitting a bimodal function is valid. The MIP also allowed to determine parameters (porosity, tortuosity, and pore connectivity) related to the hydraulic conductivity other than mercury retention curves (MRCs). Unimodal and bimodal of both vG and PDI type functions were applied using the LABROS SoilView Analysis software.

2 | MATERIALS AND METHODS

2.1 | Materials

Two rock types and three dense soil clod samples (subsoil horizons including soil parent material) were investigated. The rocks tested are the lithotypes C and M, both belonging to the Calcarenite di Gravina Formation (Andriani & Walsh, 2007). They were collected in two quarries, "Le Tufarelle," located in Canosa di Puglia (41°09′4.85″ N, 15°59′24.92″ E), and "Caprocetta," located in Massafra (40°33′29.25″ N, 17°08′32.83″ E), both in the Apulia region, southern Italy. The lithotypes C and M are hereinafter named Rock 1 and Rock 2, respectively. The rocks are characterized by a rigid structure consisting of clasts bound to each other by the carbonate cement.

The soil clods are Haplic Regosols, haRG, according to FAO classification scheme, WRB (IUSS, 2014) developed from glacial till, collected in northeastern Germany (Holzendorf, 53°22′45″ N, 13°47′11″ E), hereinafter named Till 1 (haRG74), Till 2 (haRG146), and Till 3. The data of Till 3 considered in this study come from Rieckh et al. (2012). These core samples were taken in intact layering (Figure 1); the loose fragments at the sample surface were detached due to core sampling in relatively dry conditions. Although the Till subsoils of the Haplic Regosols are relatively dense and calcaric, they still differ from calcareous porous rocks with respect to rigidity.

2.2 | Methods

The hydraulic conductivity was measured with EVA, QSC, and DMSTF methods. The WRC was determined by using EVA, QSC, ST, and PC methods. While EVA and QSC methods were able to measure both $\theta(h)$ and $K(h)$ data, the ST and PC methods measured the WRCs only, different from the DMSTF, which is capable to determine the hydraulic conductivity only (Table 1).
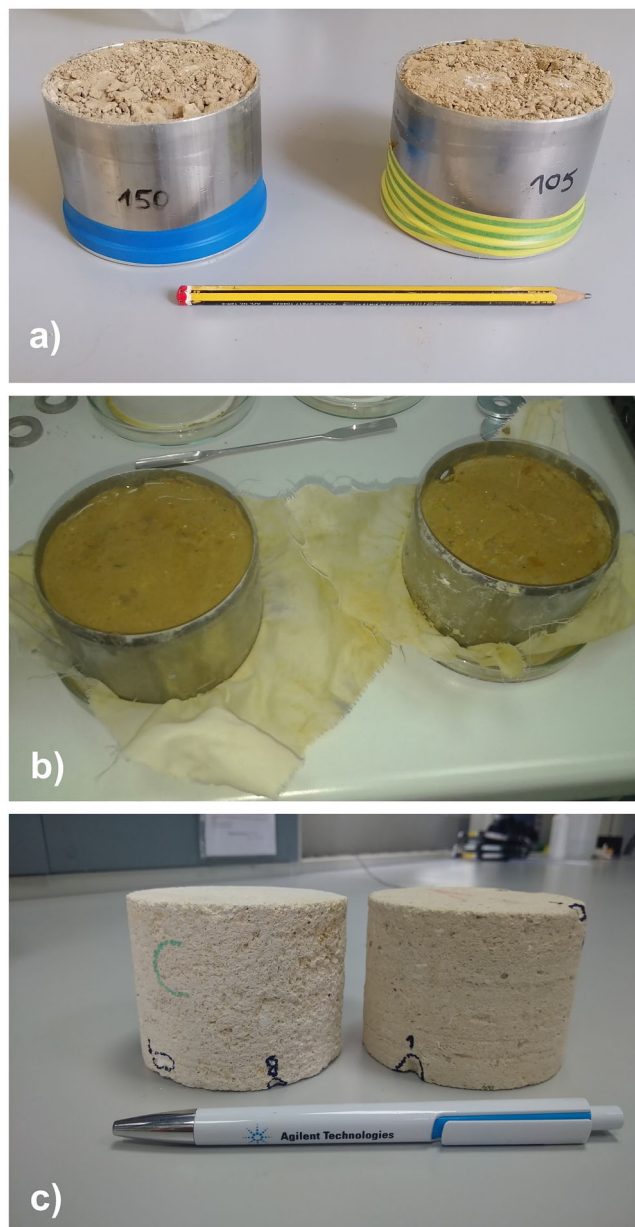
FIGURE 1 Tested samples: soil clods before (a) and after (b) the quasi-steady centrifuge (QSC) test; (c) calcareous porous rock samples.

The tested rock samples belong to the same core sample, initially 25 cm long, extracted from a unique block. Moreover, the volumes of the samples used for both EVA and QSC methods are greater than the measured representative elementary volume (REV), which is 111.54 cm^3 and 51.92 cm^3 for Rock 1 and Rock 2, respectively (Table 1).

2.2.1 | Mercury intrusion porosimetry

A Micromeritics Autopore IV 9500 porosimeter (Abell et al., 1999; Sun & Cui, 2020) was used to carry out the MIP test in order to measure the pore size distribution, the porosity

TABLE 1 Scheme of experimental tests performed by different methods (evaporation [EVA], quasi-steady centrifuge (QSC), mercury intrusion porosimetry [MIP], suction table [ST], pressure chambers [PC], and double-membrane steady-through flow [DMSTF]) to measure the retention and hydraulic conductivity curves.

EVA[a][b]	QSC[a][b]	MIP[c]	ST[a]	PC[a]	DMSTF[b]
Rock 1	Rock 1	Rock 1	Till 3[d]	Till 3[d]	Till 3[d]
Rock 2	Rock 2	Rock 2			
	Till 1	Till 1			
	Till 2	Till 2			

[a]Water retention curve (WRC).
[b]Hydraulic conductivity curve.
[c]Mercury retention curve (MRC).
[d]Data in Rieckh et al. (2012).

(Φ_{MIP} [dimensionless]), and tortuosity (τ [dimensionless]), and to determine the pore connectivity (χ [dimensionless]) of both rocks and soils (Turturro et al., 2021). For the MIP test, the Rock 1 and Rock 2 samples were hand-cut to form a parallelepiped with 1 cm square base and 2-cm high from the core sample used for QSC test. Instead, the soil clod samples, Till 1 and Till 2, were irregularly shaped being manually prepared using a knife and a scalpel, in order to obtain an approximate volume of 2 cm^3. For the structural characteristics of the samples, the porosity in laboratory (Φ [dimensionless]), was determined by subtracting to 1 the ratio of the bulk density (ρ_b) to the particle density (ρ_p) before (Φ_b) and after (Φ_a) the QSC tests. The tortuosity, that is, the ratio of the effective path length and the straight length between two points in the direction of the flow (Kutilek, 2004), was measured directly by means of MIP (τ_{MIP}), for all samples except for Till 3. Moreover, the tortuosity was also inferred by the Φ value applying the Bruggeman relation (da Silva et al., 2022) in order to compare the values before (τ_b) and after (τ_a) the QSC tests. The values of pore connectivity (χ_b), were determined as the inverse of τ_b (Table 2).

The MIP method assumes that the mercury pressure P (M L^{-1} T^{-2}) is related to the cylindrical pore diameter by the Washburn (1921) equation as:

$$P = \frac{-4\sigma_{Hg}\cos\left(\gamma_{Hg}\right)}{d} \quad (2)$$

where σ (M T^{-2}) is the mercury surface tension (0.559 M L T^{-2} L^{-1}), γ (°) is the mercury contact angle, ranging from 133° to 140°, and d (L) is the pore diameter.

2.2.2 | Evaporation

The EVA method (Wind, 1968) was used to measure θ, h, and K values within 1.5 and 2.8 pF range (pF = $-\log |h|$ with h expressed in cm). Needle tensiometers (SDEC France; Young & Sisson, 2002) were inserted into three equidistant

TABLE 2 Physical and textural properties of rock and soil clod samples: particle density, ρ_p; porosity measured by mercury intrusion porosimetry (MIP), Φ_{MIP} (dimensionless); bulk density, gravimetric porosity (dimensionless), tortuosity, pore connectivity, before (ρ_b, Φ_b, τ_b, χ_b) and after (ρ_a, Φ_a, τ_a, χ_a) the runs of the quasi-steady centrifuge (QSC) tests, respectively; clay (<0.002 mm), silt (0.063–0.002 mm) and sand (2–0.063 mm) (Rieckh et al., 2012).

Tested Sample	ρ_p (g/cm^3)	ρ_b (g/cm^3)	ρ_a (g/cm^3)	Φ_{MIP} (−)	Φ_b (−)	Φ_a (−)	τ_{MIP} (−)	τ_b (−)	τ_a (−)	χ_b (−)	χ_a (−)	Clay (%)	Silt (%)	Sand (%)
Rock 1	2.65	1.50	1.50	0.40	0.43	0.43	3.86	1.52	1.52	0.65	0.65	n.a.	n.a.	n.a.
Rock 2	2.65	1.56	1.56	0.36	0.41	0.41	4.47	1.56	1.56	0.64	0.64	n.a.	n.a.	n.a.
Till 1	2.64	1.76	1.98	0.23	0.33	0.25	6.89	1.74	2	0.57	0.5	11.8	26.7	61.4
Till 2	2.64	1.76	1.98	0.25	0.33	0.25	6.89	1.74	2	0.57	0.5	11.8	26.7	61.4
Till 3	2.64	1.76		0.25	0.33			1.74		0.57		11.8	26.7	61.4

holes drilled along the sample, previously laterally sealed by epoxy resin and saturated under vacuum. The samples, closed at the bottom by parafilm lid and placed on loading cell, were subjected to free EVA. The changes in time of sample weight and matric potential, due to water content decrease for EVA, were recorded. The $\theta(h)$ was calculated by using an iteration procedure that allowed to correct the a priori supposed WRC by using the sample weight and pressure head measurements recorded during the test. The $K(h)$, instead, was calculated by the Darcy's law applying the Instantaneous Profile Method (Watson, 1966). These calculations were performed by the program package METRONIA. The tested rock samples, 7.8 cm in diameter and 12 cm in height, were obtained by disc-cutting the cores previously drilled from the blocks collected in the quarries.

2.2.3 | Quasi-steady centrifuge

The QSC method, described in detail by Caputo and Nimmo (2005), was used to test both the core samples of rocks, extracted from the blocks, and of soils, collected in the field with a cylindrical steel sampler. All the tested samples were 7.8 cm in diameter and 6 cm in height. The QSC method is based on an experimental apparatus that fits into a swinging centrifuge bucket. The apparatus consists of a reservoir that, resting on the sample, regulates the inflow rate by means of a layer of different granular material (i.e., silica sand, diatomaceous earth, bentonite, and silica flour) laid at the bottom of the reservoir. Below the sample there is a ceramic plate that lies on an outflow disk placed at a certain distance from the bottom of the centrifuge bucket in order to avoid that water collected during the run can reach the sample by changing its moisture. Whenever the sample reaches the steadiness in terms of water content (θ), an external tensiometer with a flat surface ceramic disc, instead of the common ceramic cup, that allows close contact between the sample's upper face and the tensiometer, measures the corresponding h value. The Darcy–Buckingham law in the centrifugal field (Turturro et al., 2020) was applied to compute the value of K for each h value:

$$q = -\frac{K(\theta)}{\rho g}\left(\frac{dh}{dr} - \rho \omega r^2\right) \qquad (3)$$

where q (L T^{-1}) is the flux density, ρ (M L^{-3}) is the water density, g (L T^{-2}) is the gravitational acceleration, ω (T^{-1}) is the angular speed, and r (L) is the distance of measurement point, fixed at sample half height, from the rotation axis.

A series of runs, corresponding to centrifugal acceleration values ranging between 230 and 2000 rpm, were carried out to achieve different water content values in the samples, and to measure K values in a wide moisture range, both for rocks and for soils.

2.2.4 | Double-membrane steady-through flow, suction table, and pressure chambers

The DMSTF method was used to measure the $K(h)$ curve by imposing a unit hydraulic gradient at 1.3, 1, 0.7, and 0 pF pressure head values (Rieckh et al., 2012). The h values were measured with two tensiometers. The sample weight, together with the h value, was recorded every 10 s in the first 30 min, every 60 s for the next 2.5 h, and every 300 s until the end of experiment.

Rieckh et al. (2012) used the ST method (Romano et al., 2002) to measure the WRCs of five soil clod samples, the data of which are considered in this study. The saturated core samples were rested above sand and kaolin clay layer of the Eijkelkamp boxes connected to a hanging water column. The negative pressure heads, which correspond to 0, 0.7, 1, 1.3, 1.7, 1.9, 2, 2.3, and 2.5 pF suction values, were applied to the core samples bottom to obtain desorption WRCs.

In order to expand the range of the WRCs of the tested soil samples, the pairs of (θ, h) values reported in Rieckh et al. (2012) obtained by using the PC (Dane & Hopmans, 2002) method for h values equal to suctions of 3, 3.7, and 4.2 pF, were also considered in this study.

2.2.5 | Data fitting

LABROS SoilView Analysis software (Peters & Durner, 2015), commercialized by the METER group, was used for fitting different models of hydraulic functions to the measured values of water content (θ), mercury content (θ_{Hg}), matric potential (h), and hydraulic conductivity (K), obtained with the abovementioned methods. This software is accurate and versatile for fitting hydraulic data by different models, both in unimodal and bimodal form, and capable of describing hydraulic behavior across the full measurement range. Four different numerical formulations were used for fitting the experimental data in order to see which one provides the best fit and allows the better description of the hydraulic behavior of the tested media.

Specifically, unimodal vG formulation (Equation 4) was initially used (Lipovetsky et al., 2020; Pertassek et al., 2015):

$$K(S_e) = K_S S_e^{\chi}\left[1 - \left(1 - S_e^{1/m}\right)^m\right]^2 \qquad (4)$$

with

$$S_e(h) = \frac{\theta(h) - \theta_r}{\theta_s - \theta_r} = \frac{1}{\left[1 + |\alpha h|^n\right]^m} \qquad (5)$$

where S_e (L^3 L^{-3}) is effective saturation, θ_s (L^3 L^{-3}) and θ_r (L^3 L^{-3}) are saturated and residual water contents, respectively, α (L^{-1}), n, and m are dimensionless empirical

shape parameters, $m = 1 - 1/n$, and χ is the pore connectivity, which is inversely proportional to the tortuosity and accounts for the correlation factors among adjacent pores (Basile et al., 2020).

In addition, bimodal formulation of vG hydraulic conductivity function (Equation 6) was used in order to capture the dual porosity of the tested media (Priesack & Durner, 2006):

$$K\left(S_e\right) = K_s \frac{\left(w_1 S_1 + w_2 S_2\right)^{\chi} \left\{ w_1 \alpha_1 \left[1 - \left(1 - S_1^{1/m_1}\right)\right]^{m_1} + w_2 \alpha_2 \left[1 - \left(1 - S_2^{1/m_2}\right)\right]^{m_2} \right\}^2}{\left(w_1 \alpha_1 + w_2 \alpha_2\right)^2} \tag{6}$$

where S_i, α_i, n_i, and m_i are the same as in Equations (4) and (5), for $i = 1$ or 2, referred to micropores or macropores regions of the tested medium, and w is the parameter that defines the division in micro- and macropores regions with $\sum w_i = 1$.

2.2.6 | Statistical analysis

LABROS SoilView Analysis software measures the root mean square error (RMSE) to evaluate the performance of the fitted model by quantifying the differences between measured (y_i) and model predicted ($\hat{y}_i$) value:

$$\text{RMSE} = \sqrt{\frac{1}{p} \sum_{i=1}^{p} \left[y_i - \hat{y}_i\right]^2} \tag{7}$$

where p is the number of data points. Moreover, the used software provides the corrected akaike information criterion (AICc) (Akaike, 1974; Hurvich & Tsai, 1989) to account for adjustable parameters in case of comparison among different models fitting the same experimental data:

$$\text{AIC}_c = 2\left(l + k\right) + \left(\frac{2k\left(k + 1\right)}{p - k - 1}\right) \tag{8}$$

where l is the likelihood function and k the number of fitting parameters. The AICc value is usually negative, and the larger it is, the more appropriate the model.

3 | RESULTS AND DISCUSSION

The MIP tests (Figure 2) show that pore size distributions for rock samples are different from those of the till samples. For the rocks, the pore diameter distribution shows two peaks that differ depending on the lithotype. Specifically, (i.e., at 0.14 and 27.5 μm for Rock 1 and 1.84 and 19.7 μm for Rock 2) with most pores in the 10- to 50-μm diameter range, while the till samples (Till 1 and Till 2) are both showing several but smaller peaks (i.e., at 0.008, 0.03–0.04, 0.4–0.8, and around 200 μm) with the majority of pores in the range 6–300 μm. Rock 1 shows a more evident bimodality than Rock 2 due to the bioclasts, responsible for the larger pores, and to the intergranular cement that contributes to the smaller pores as compared to Rock 2 (Andriani & Walsh, 2010). The measurement range of pore diameters detectable by MIP was between about 0.003 and 420 μm. Thus, all pore sizes that were not detected by MIP could not be accounted for in the porosity calculated from MIP (Φ_{MIP}). For the relatively small clod samples from the till, much of the cracks and macropores are excluded such that the porosity (Φ), observed on larger sized samples (Rieckh et al., 2012) resulted larger (Table 1). Also for the rock samples, the sample-size-dependent porosity difference showed that macropores and micropores are not detected by MIP such that Φ value estimated on larger samples was higher than Φ_{MIP}. In fact, all the samples exhibit a value of porosity obtained by MIP (Φ_{MIP}), which is smaller than Φ (Table 1) due to the limited pore range investigable by MIP test. According to Kutílek (2004), who considered the pore size of 15 μm as the boundary value between textural and structural pores, the peaks on the right of the graph in Figure 2 represent the modal pore size of the structural or interpedal pores, while the peaks on the left indicate the modal pore size of the textural or intrapedal pores. The water retention and hydraulic conductivity curves of porous rocks and soil clods cover different ranges (Figure 3; Tables 3 and 4).

All the graphs in Figure 3 show that for rocks there are not much data points close to saturation because, during the preparatory operations needed to start the EVA and QSC tests, the samples easily lose water under the action of gravity, differently than soils that have clayey silt texture. Instead, the MRCs have not points close to saturation because the minimum pressure achievable with the Micromeritics Autopore IV 9500 micro-porosimeter equals a pressure head value of $-h = 1.58$ pF.

Looking at WRCs of calcareous rocks (Figure 3a), it is observed that the θ_s value measured by the EVA method ($\theta_s = 0.38$ cm³ cm⁻³ and $\theta_s = 0.36$ cm³ cm⁻³ for Rock 1 and Rock 2, respectively; see Table 3) is lower than Φ (Table 1). By
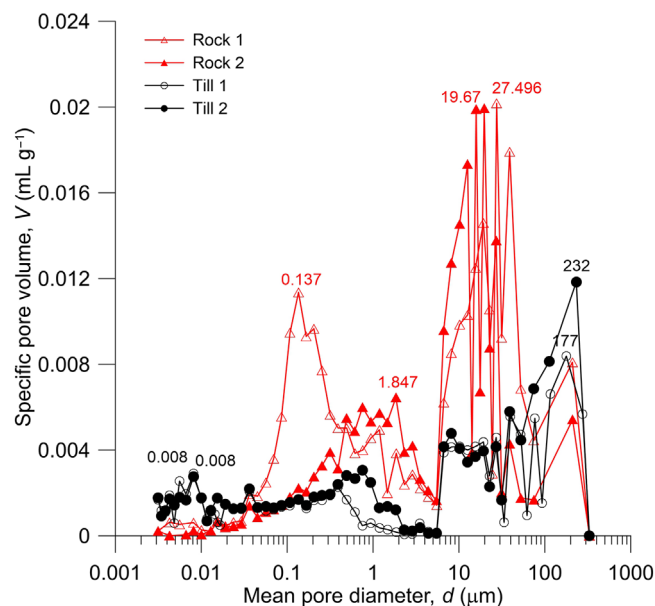
FIGURE 2 Pore size distribution measured by mercury intrusion porosimetry (MIP) for both calcareous rocks and soil clods.

TABLE 3 Minimum and maximum values of liquid content, θ_{min} (cm^3 cm^{-3}) and θ_{max} (cm^3 cm^{-3}), and matric potential, h_{min} (pF) and h_{max} (pF), measured by evaporation (EVA), quasi-steady centrifuge (QSC), mercury intrusion porosimetry (MIP), suction table (ST), and pressure chambers (PC) methods.

Method	Sample	θ_{min}	h_{min}	θ_{max}	h_{max}
EVA	Rock 1	0.153	2.75	0.383	0.26
	Rock 2	0.061	2.65	0.318	1.15
QSC	Rock 1	0.198	2.68	0.420	1.09
	Rock 2	0.135	2.68	0.408	1.02
	Till 1	0.180	2.02	0.194	1.12
	Till 2	0.184	2.29	0.194	0.20
ST	Till 3	0.204	2.5	0.304	0
MIP	Rock 1	0.0003[a]	6.62[a]	0.38[a]	1.58[a]
	Rock 2	0.0003[a]	6.62[a]	0.35[a]	1.58[a]
	Till 1	0.0003[a]	6.62[a]	0.24[a]	1.58[a]
	Till 2	0.0003[a]	6.62[a]	0.25[a]	1.58[a]
PC	Till 3	0.11	4.2	0.212	3

[a]Volumetric mercury content, θ_{Hg}.

considering that all the pores of the rocks are interconnected and continuous, as Andriani and Walsh (2009) demonstrated by reaching the full saturation of these rocks, the abovementioned difference is due to the water loss by gravity when handling the samples under the saturation conditions and to the optimization of the a priori supposed WRC performed by the Metronia program. By contrast, for the rocks, the difference between Φ (Table 1) and θ_s measured by QSC ($\theta_s = 0.43$ cm^3 cm^{-3} and $\theta_s = 0.41$ cm^3 cm^{-3} for Rock 1 and Rock 2, respectively; see Table 3) is zero, making the QSC the only

TABLE 4 Minimum and maximum values of hydraulic conductivity, K_{min} (cm d^{-1}) and K_{max} (cm d^{-1}), and matric potential, h_{min} (pF) and h_{max} (pF), measured by evaporation (EVA), quasi-steady centrifuge (QSC), and double-membrane steady-through flow (DMSTF) methods.

Method	Sample	K_{min}	h_{min}	K_{max}	h_{max}
EVA	Rock 1	0.002	2.68	0.214	1.58
	Rock 2	0.005	2.61	0.788	1.73
QSC	Rock 1	0.083	2.66	44.614	0.94
	Rock 2	0.025	2.68	25.063	1.02
	Till 1	0.003	2.02	0.344	0.73
	Till 2	0.003	2.29	0.427	0.30
DMSTF	Till 3	1.01	1.30	89.5[a]	0

[a]Rieckh et al. (2012).

method capable to provide θ_s value equal to the porosity. This is due to the continuous supply of water to the sample from the upper reservoir of the QSC experimental apparatus. Also, the WRCs of the rocks obtained by the EVA method clearly show a gap in the wet range, for $-h \leq 1.4$ pF. In that range, because of the handling of the saturated samples in order to close their bottom part by parafilm lids, the larger pores easily lose water by gravity that acts more rapidly than EVA.

In the middle range, which corresponds to medium-size pores of the rocks, the highest θ values measured by QSC are higher than those measured by EVA, meaning that the QSC is able to provide data points closer to saturation compared to the EVA method. In addition, the curves obtained for the same rock by EVA and QSC methods diverge for $-h \geq 1.7$ pF and $\theta \leq 0.35$ cm^3 cm^{-3}, showing a steeper EVA curve than the QSC one, especially for Rock 2. The discrepancy between the two curves is due to the differences in sample size, physical process, boundary conditions, calculation methods, simplifying assumptions, and measuring θ and h values by the two methods. In fact, the EVA method measures the pair (θ, h), while they change quasi-continuously, being it a transient flow conditions method, whereas the QSC method records them when θ reaches the steadiness (quasi-steady state condition). The bimodal behavior of rock WRCs is clearly shown in those measured by QSC and MIP.

The soils WRCs measured by the QSC method (Figure 3b) have no S-shape due to the collapse of larger pores caused from the soil compaction that occurs during the centrifugation (Khanzode et al., 2002; Nimmo & Akstin, 1988; Omoregie, 1988). The compaction affects nonrigid soils, although they are dense. Unlike, the rocks are not affected by the compaction because of their rigid structure, even if their bulk density, ρ_b, is lower than soils. The θ_s measured by Rieckh et al. (2012) for soil clods equals 0.309 cm^3 cm^{-3} and is lower than both the soil porosity ($\Phi = 0.332$) and the θ_s measured for rocks. This is consistent with the higher ρ_b of the soils compared to the
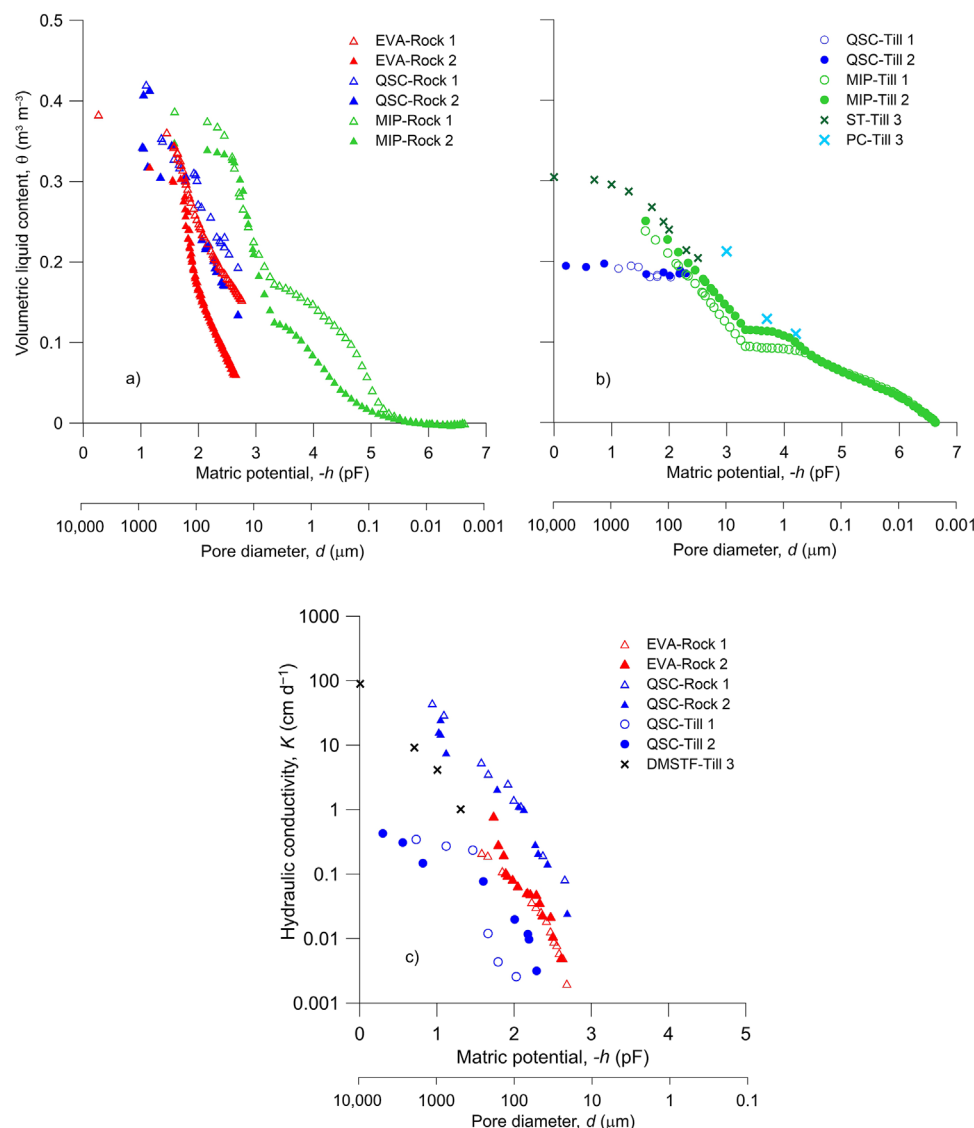
FIGURE 3 Water retention curves (WRCs) measured by suction table (ST), evaporation (EVA), quasi-steady centrifuge (QSC) and pressure chambers (PC) methods, and mercury retention curves (MRCs) measured by mercury intrusion porosimetry (MIP) for rocks (a) and soils (b); (c) hydraulic conductivity curves obtained by EVA, QSC and double membrane steady-through flow (DMSTF) methods of calcareous rocks and soil clods.

rocks as discussed in Rieckh et al. (2012) (Table 1). The soils WRCs measured by both ST and QSC methods cover the h range close to saturation. Particularly, the ST is able to capture the soil $\theta(h)$ curve at $h = 0$ pF. Among the direct methods, the PC method is the only one that reached the lowest h value ($-h = 4.2$ pF), while the EVA method is the sole one that measured the lowest θ value ($\theta = 0.05$ cm^3 cm^{-3}). Overall, the QSC method, on varying the operating conditions (type and thickness of granular materials, run duration, and rpm), allows to obtain many more points of the WRC capable to cover the entire moisture range.

By comparing the two investigated media, the soils WRCs and MRCs are less steep than for rocks (Figure 3a,b), because the soils have heterogeneous pore size distribution compared

to rocks. For Till 3, the θ value at $-h = 3$ pF measured by PC is higher than those expected for the rocks WRCs due to the effect of the clay content in the soil (Rieckh et al., 2012).

The $K(h)$ curves, depicted in Figure 3c, highlighted that data points obtained by the QSC method are shifted upward and widespread on the left, reaching higher h and K values compared to those measured by EVA. This is because during the QSC tests, the upper surface of the samples is continuously supplied by water, while the EVA method is not reliable for pressure head values ranging between 0 and -1.7 pF. Therefore, the gap between the two (K, h) curves obtained by QSC and EVA methods is due to different measurement condition in the mentioned methods: the QSC allows measuring K and h values when the sample reaches the θ steadiness, whereas

TABLE 5 Values of fitted parameters and statistical analysis for the van Genuchten (vG) and Peters Durner Iden (PDI) unimodal and bimodal rocks water retention curves (WRCs) and hydraulic conductivity function measured by evaporation (EVA) method.

Parameter(unit)	Rock 1				Rock 2			
	Unimodal vG	BimodalvG	UnimodalPDI	BimodalPDI	UnimodalvG	BimodalvG	UnimodalPDI	BimodalPDI
α (1 cm^{-1})	0.0315 0.0158[a]	–	0.0320 0.0320[a]	–	0.0179 0.015[a]	–	0.0179 0.015[a]	–
n	1.317 1.457[a]	–	1.303 1.363[a]	–	1.777 1.906	–	1.904 1.906[a]	–
θ_r ($cm^3\,cm^{-3}$)	0.001	0.001	0.001	0.001	0.001	0.001	0.001	0.001
θ_s ($cm^3\,cm^{-3}$)	0.38	0.38	0.38	0.38	0.318	0.318	0.318	0.318
w_2	–	0.239	–	0.093	–	0.090	–	0.756
α_1 (1 cm^{-1})	–	0.0207 0.0184[a]	–	0.0457 0.0132[a]	–	0.0149 0.00823[a]	–	0.0135 0.00824[a]
α_2 (1 cm^{-1})		0.14 0.0123[a]		0.0168 0.0181[a]		0.5 0.015[a]		0.0743 0.0150[a]
n_1	–	1.615 3.933[a]	–	1.010 1.298[a]	–	2.097 1.905[a]	–	2.828 1.903[a]
n_2		1.010 1.315[a]		2.333 4.148[a]		1.010 7.895[a]		1.010 7.898[a]
$RMSE_\theta$	0.0108 0.013[a]	0.0065 0.0025[a]	0.0110 0.0092[a]	0.0043 0.0025[a]	0.0144 0.0126[a]	0.0115 0.0047[a]	0.0145 0.012[a]	0.0103 0.0047[a]
$RMSE_K$	0.6578 1.1634[a]	0.5409 0.16[a]	0.6351 0.1339[a]	0.1722 0.149[a]	1.2486 1.4735[a]	0.7612 0.4655[a]	0.2476 0.395[a]	0.1754 0.1329[a]
AICc	−811 −738[a]	−871 −1072[a]	−810 −884[a]	−1003 −1075[a]	−825 −791[a]	−894 −964[a]	−823 −791[a]	−968 −964[a]

Abbreviations: AICc, akaike information criterion; RMSE, root mean square error.

[a]Values obtained not fixing the tortuosity value but considering it as a free parameter.

TABLE 6 Values of fitted parameters and statistical analysis for the van Genuchten (vG) and Peters Durner Iden (PDI) unimodal and bimodal rocks water retention curves (WRCs) and hydraulic conductivity functions measured by quasi-steady centrifuge (QSC) method.

Parameter (unit)	Rock 1				Rock 2			
	Unimodal vG	Bimodal vG	Unimodal PDI	Bimodal PDI	Unimodal vG	Bimodal vG	Unimodal PDI	Bimodal PDI
α (1 cm^{-1})	0.0286 / 0.0528[a]	– / –	0.0577 / 0.0602[a]	– / –	0.0256 / 0.0226[a]	– / –	0.0420 / 0.0231[a]	– / –
n	1.324 / 1.245[a]	– / –	1.213 / 1.208[a]	– / –	1.430 / 1.472[a]	– / –	1.327 / 1.465[a]	– / –
θ_r (cm^3 cm^{-3})	0.001	0.001	0.001	0.001	0.001	0.001	0.001	0.001
θ_s (cm^3 cm^{-3})	0.431	0.431	0.431	0.431	0.408	0.41	0.41	0.41
w_2	–	0.194	–	0.889	–	0.108	–	0.262
α_1 (1/cm)	–	0.00903 / 0.0106[a]	–	0.0551 / 0.0127[a]	–	0.0122 / 0.00141[a]	–	0.1414 / 0.0014[a]
α_2 (1/cm)	–	0.0641 / 0.0549[a]	–	0.0234 / 0.0567[a]	–	0.1402 / 0.022[a]	–	0.0108 / 0.022[a]
n_1	–	1.404 / 1.373	–	15 / 1.332[a]	–	1.597 / 2.478[a]	–	1.136 / 2.479[a]
n_2	–	5.587 / 7.713[a]	–	1.256 / 8.816[a]	–	15 / 1.949[a]	–	2.844 / 1.949[a]
RMSE$_\theta$	0.0186 / 0.0138[a]	0.0087 / 0.0083[a]	0.0124 / 0.0124[a]	0.0086 / 0.0081[a]	0.0184 / 0.0070[a]	0.0159 / 0.0049[a]	0.0184 / 0.0068[a]	0.0147 / 0.0049[a]
RMSE$_K$	0.4747 / 0.3546[a]	0.2934 / 0.2275[a]	0.1749 / 0.159[a]	0.1799 / 0.1804[a]	0.5931 / 0.479[a]	0.4039 / 0.1957[a]	0.3166 / 0.2835[a]	0.2553 / 0.2041[a]
AICc	−313 / −184[a]	−356 / −197[a]	−352 / −188[a]	−367 / −198[a]	−283 / −144[a]	−294 / −143[a]	−298 / −145[a]	−305 / −143[a]

Abbreviations: AIC$_C$, akaike information criterion; RMSE, root mean square error.

[a]Values obtained not fixing the tortuosity value but considering it as a free parameter.

TABLE 7 Values of fitted parameters and statistical analysis for the van Genuchten (vG) and Peters Durner Iden (PDI) unimodal and bimodal rocks mercury retention curves (MRCs) inferred by mercury intrusion porosimetry (MIP) method.

Parameter (unit)	Rock 1				Rock 2			
	Unimodal vG	Bimodal vG	Unimodal PDI	Bimodal PDI	Unimodal vG	Bimodal vG	Unimodal PDI	Bimodal PDI
α (1 cm^{-1})	0.00358 / 0.00375[a]	–	0.00465 / 0.00489[a]	–	0.002 / 0.00207[a]	–	0.00205 / 0.00213[a]	–
n	1.349 / 1.347[a]	–	1.273 / 1.263[a]	–	1.546 / 1.543[a]	–	1.526 / 1.522[a]	–
θ_r (cm^3 cm^{-3})	0.001	0.001	0.001	0.001	0.001	0.001	0.001	0.001
θ_s (cm^3 cm^{-3})	0.404	0.404	0.404	0.404	0.364	0.364	0.364	0.364
w_2	–	0.7	–	0.302	–	0.912	–	0.196
α_1 (1 cm^{-1})	–	0.00002 / 0.00258[a]	–	0.00248 / 0.00258[a]	–	0.00007 / 0.00182[a]	–	0.00136 / 0.00203[a]
α_2 (1 cm^{-1})		0.00248 / 0.00002[a]		0.00002 / 0.00002[a]		0.00150 / 0.00137[a]		0.00181 / 0.00134[a]
n_1	–	2.439 / 2.166[a]	–	2.226 / 2.176[a]	–	1.961 / 1.455[a]	–	6.513 / 1.389[a]
n_2		2.214 / 2.462[a]		2.393 / 2.416[a]		2.964 / 7.591[a]		1.392 / 6.776[a]
RMSE$_{\theta Hg}$	0.0228 / 0.228[a]	0.0049 / 0.0052[a]	0.0199 / 0.0198[a]	0.0047 / 0.0050[a]	0.0142 / 0.0141[a]	0.0048 / 0.0088[a]	0.0142 / 0.014[a]	0.0071 / 0.073[a]
AICc	–396 / –397[a]	–553 / –547[a]	–411 / –411[a]	–556 / –549[a]	–464 / –465[a]	–577 / –509[a]	–464 / –465[a]	–534 / –530[a]

Abbreviations: AIC$_C$, akaike information criterion; RMSE, root mean square error.

[a]Values obtained not fixing the tortuosity value but considering it as a free parameter.

TABLE 8 Values of fitted parameters values and statistical analysis for the van Genuchten (vG) and Peters Durner Iden (PDI) unimodal and bimodal soils water retention curves (WRCs) and hydraulic conductivity functions measured by quasi-steady centrifuge (QSC) method.

Parameter(unit)	Till 1				Till 2			
	Unimodal vG	Bimodal vG	Unimodal PDI	Bimodal PDI	Unimodal vG	Bimodal vG	Unimodal PDI	Bimodal PDI
α (1 cm^{-1})	0.0479 0.5[a]	–	0.1393 0.5[a]	–	0.0208 0.5[a]	–	0.1634 0.5[a]	–
n	1.538 1.196[a]	–	1.297 1.157[a]	–	1.509 1.172[a]	–	1.187 1.123[a]	–
θ_r (cm^3 cm^{-3})	0.037	0.037	0.037	0.037	0.037	0.037	0.037	0.037
θ_s (cm^3 cm^{-3})	0.309	0.309	0.309	0.309	0.309	0.309	0.309	0.309
w_2	–	0.423	–	0.934	–	0.359	–	0.413
α_1 (1 cm^{-1}) α_2 (1 cm^{-1})	–	0.00798 0.5[a] 0.0868 0.0603[a]	–	0.5 0.042[a] 0.0126 0.0051[a]	–	0.00447 0.5[a] 0.3060 0.00002[a]	–	0.00411 0.00004[a] 0.5 0.5[a]
n_1 n_2	–	15 8.44[a] 15 1.073[a]	–	7.891 2.886[a] 1.01 15[a]	–	15 3.993[a] 15 4.865[a]	–	15 5.363[a] 4.584 4.296[a]
RMSE$_\theta$	0.0368 0.0146[a]	0.0091 0.003[a]	0.0227 0.0155[a]	0.0041 0.309[a]	0.0645 0.0415[a]	0.0410 0.0259[a]	0.0510 0.0429[a]	0.0270 0.0266[a]
RMSE$_K$	0.9672 0.2895[a]	0.5031 0.0178[a]	0.4865 0.1689[a]	0.1405 0.0193[a]	0.8992 0.3336[a]	1.5373 0.0043[a]	0.9783 0.2578[a]	1.5018 0.0043[a]
AICc	−103 −70[a]	−124 −75[a]	−118 −69[a]	−53 −41[a]	−105 −64[a]	−97 −58[a]	−101 −64[a]	−100 −58[a]

Abbreviations: AIC$_C$, akaike information criterion; RMSE, root mean square error.

[a]Values obtained not fixing the tortuosity value but considering it as a free parameter.

TABLE 9 Values of fitted parameters values and statistical analysis for the van Genuchten (vG) and Peters Durner Iden (PDI) unimodal and bimodal soils water retention curves (WRCs) and hydraulic conductivity functions measured by the suction table (ST), pressure chambers (PC), and double-membrane steady-through flow (DMSTF) methods.

Parameter (unit)	Till 3			
	Unimodal vG	Bimodal vG	Unimodal PDI	Bimodal PDI
α (1 cm^{-1})	0.0337 0.0369[a]	–	0.0683 0.0608[a]	–
n	1.192 1.185[a]	–	1.068 1.073[a]	–
θ_r (cm^3 cm^{-3})	0.037	0.037	0.037	0.037
θ_s (cm^3 cm^{-3})	0.309	0.309	0.309	0.309
w_2	–	0.5	–	0.587
α_1 (1 cm^{-1}) α_2 (1 cm^{-1})	–	0.00038 0.0624	–	0.0665 0.00039
n_1 n_2	–	1.510 1363	–	1.383 1.336
RMSE$_\theta$	0.0117 0.0117[a]	0.0089	0.0107 0.0106[a]	0.0092
RMSE$_K$	0.337 0.1683[a]	0.2239	0.5368 0.0602[a]	0.2152
AICc	−147 −110[a]	−147	−141 −113[a]	−141

Abbreviations: AIC$_C$, akaike information criterion; RMSE, root mean square error.

[a]Values obtained not fixing the tortuosity value but considering it as a free parameter.

TABLE 10 Values of fitted parameters values and statistical analysis for the van Genuchten (vG) and Peters Durner Iden (PDI) unimodal and bimodal soils mercury retention curves (MRCs) for data inferred by mercury intrusion porosimetry (MIP) method.

Parameter (unit)	Till 1				Till 2			
	Unimodal vG	**Bimodal vG**	**Unimodal PDI**	**Bimodal PDI**	**Unimodal vG**	**Bimodal vG**	**Unimodal PDI**	**Bimodal PDI**
α (1 cm^{-1})	0.035 / 0.035[a]	– / –	0.3186 / 0.3186[a]	– / –	0.0209 / 0.0209[a]	– / –	0.1784 / 0.1784[a]	– / –
n	1.317 / 1.317[a]	– / –	1.099 / 1.099[a]	– / –	1.311 / 1.311[a]	– / –	1.090 / 1.090[a]	– / –
θ_r (cm^{3}cm^{-3})	0.037	0.037	0.037	0.037	0.037	0.037	0.037	0.037
θ_s (cm^{3}cm^{-3})	0.309	0.309	0.309	0.309	0.309	0.309	0.309	0.309
w_2	–	0.635	–	0.866	–	0.199	–	0.942
α_1 (1 cm^{-1})	–	0.00431 / 0.0893[a]	–	0.0342 / 0.0146[a]	–	0.0208 / 0.0208[a]	–	0.006 / 0.5[a]
α_2 (1 cm^{-1})		0.0893 / 0.00431[a]		0.00001 / 0.5		0.00003 / 0.00003[a]		0.5 / 0.006[a]
n_1	–	1.354 / 1.356[a]	–	1.445 / 1.978[a]	–	1.480 / 1.480[a]	–	2.269 / 1.017[a]
n_2		1.356 / 1.354[a]		1.01 / 1.01[a]		2.182 / 2.182[a]		1.017 / 2.269[a]
RMSE$_{\theta Hg}$	0.0153 / 0.0153[a]	0.0148 / 0.0148[a]	0.0118 / 0.0118[a]	0.0059 / 0.0082[a]	0.0174 / 0.0174[a]	0.0128 / 0.0128[a]	0.0071 / 0.0071[a]	0.0042 / 0.0041[a]
AICc	−497 / −497[a]	−494 / −494[a]	−529 / −529[a]	−605 / −566[a]	−433 / −433	−460 / −460[a]	−531 / −531[a]	−579 / −579[a]

Abbreviations: AIC$_C$, akaike information criterion; RMSE, root mean square error.

[a]Values obtained not fixing the tortuosity value but considering it as a free parameter.

the EVA method measures K and h values while they continuously change. For rocks, the QSC method is the only one able to measure the highest K and lowest θ values. The QSC method allows us to capture the bimodality of the curves, more evident for Rock 2 and Till 2.

The $K(h)$ curves of the rocks obtained by the QSC method overlap, while those obtained by EVA deviate for $-h \leq 1.9$ pF, by showing higher K values for Rock 2 than for Rock 1 for the same h value. This is because the Rock 2, which has grains and pores smaller than Rock 1, traps more water for the same matric potential compared to Rock 1. The maximum h measured value, the closest to the saturation, reached for Rock 1 is higher than for Rock 2, with both methods pointing out that the measured data capture larger pores of Rock 1 compared to Rock 2. This is consistent with the higher Φ and Φ_{MIP} values of Rock 1 with respect to Rock 2 (Table 1). In fact, calcareous concretions, macropores and cracks, at the interface between the concretions and surrounding medium, contribute to higher porosity of Rock 1, as observed by optical petrographic microscopy on thin sections (Ravina & Magier, 1984). The EVA method fails in the near-saturation range where the K value is highest, leading to very small hydraulic gradients that cannot be determined with sufficient accuracy (Wendroth & Šimůnek, 1999). In the present study, the EVA method was not applied to the soil clod samples; we assumed that the measurements reported in Rieckh et al. (2012), obtained by using the DMSTF method, may be considered complementary with those determined with QSC one. Because the samples' volume of the tested rocks is greater than the REV, the outcomes can be considered representative of the whole, hence ideally ascribable to the same sample. However, slight differences in terms of results may be due to differences in the individual samples (Caputo & Nimmo, 2005).

The soils $K(h)$ curves measured by QSC (Figure 3c) are below those measured by the DMSTF method because of pores collapse due to compaction, which occurs during the QSC test. With respect to other methods, the QSC provides relatively accurate $K(h)$ measurements in larger range of h and allows to capture the bimodal behavior of the tested rocks not found by EVA and DMSTF methods. In fact, only the hydraulic conductivity curves measured by QSC show an inflection point for both the rock samples, highlighting a bimodal behavior that is consistent with the results of the MIP tests (Figure 2).

By comparing the two investigated media, the $K(h)$ curve of Till 2 shows the maximum h value measured by QSC ($-h = 0.3$ pF) that is closer to saturation than Rock 1 ($-h = 0.94$ pF), because soils have higher percentage of small pores (as shown in Figure 2) that entrap more water compared to larger pores (van den Berg et al., 2009).

The QSC method captures the flow in an additional pore system, specifically that related to the larger pores compared

to EVA and DMSTF methods (Figure 3). However, the QSC method has a crucial weakness related to the centrifugal force that can cause a compaction of soil pores, being them nonrigid (Horn et al., 2014; Schlüter et al., 2016). This fact affects the soil structure and consequently the hydraulic characteristics as corroborated by literature (Khanzode et al., 2002; Nimmo & Akstin, 1988; Omoregie, 1988). The soil's volume decreases due to compaction and causes structural deformation implying a change of bulk density with respect to the in situ value, ρ_b (Fu et al., 2011). In fact, the ρ_b value for the soil samples increased from $\rho_b = 1.76$ g cm^{-3} to $\rho_a = 1.98$ g cm^{-3} (i.e., the bulk density after a series of runs during QSC tests).

The tortuosity values, both those measured by MIP and those inferred as the reciprocal of the porosity, resulted in higher values for soils than for rocks (Table 2). This is due to fact that the soils pore system, differently to the rocks, evolves over time being related to pedogenesis and to biologic factors such as root properties, plant species, and soil organic matter composition (Musso et al., 2019). In addition, cultivation condition, such as tillage and/or no tillage directly affect the connectivity of pores and consequently the tortuosity of flow path by impacting hydraulic properties (Ghambarian et al., 2023). The tortuosity, τ_b, directly measured by MIP (Table 1), allowed us to derive the pore connectivity before the QSC test (χ_b), which was greater for rocks than for soils ($\chi_b = 0.65$ for Rock 1, $\chi_b = 0.64$ for Rock 2, and $\chi_b = 0.57$ for both the till samples). As shown in Table 1, the structural characteristics (bulk density, porosity, tortuosity, and pore connectivity), determined before and after the QSC tests, are constant for both the tested rocks unlike the soils, confirming that the QSC method modifies the structure of nonrigid media such as the investigated soils that are not rigid although highly dense. Moreover, soil compaction causes the change in pore size distribution by decreasing both the number and the volume of the larger pores (van den Berg et al., 2009) and, consequently, the Φ value that varied from 0.33 to 0.25, after the centrifugation (Table 1). Therefore, the sample height decreased by about 1 cm within the cylindrical sampler by making the reservoir, which rests above the sample itself in the centrifuge bucket, unstable. Compaction was observed, especially in the central part of the soil sample, because of the friction effect between the sample and the sampler edge. Therefore, the decrease in sample height leads to the loss of contact between filter membrane at the bottom of the reservoir and the sample itself, by causing the filter membrane to break under the centrifugal force. Another aspect that makes the QSC method not effective for soil is the difficulty in obtaining a good contact between the sample upper surface, distorted under the centrifugal force effect, and the tensiometer (Turturro et al., 2021).

Even though the QSC method is not suitable for soils, it has the advantage of allowing fast measurement of K values with respect to the gravity-driven steady methods for
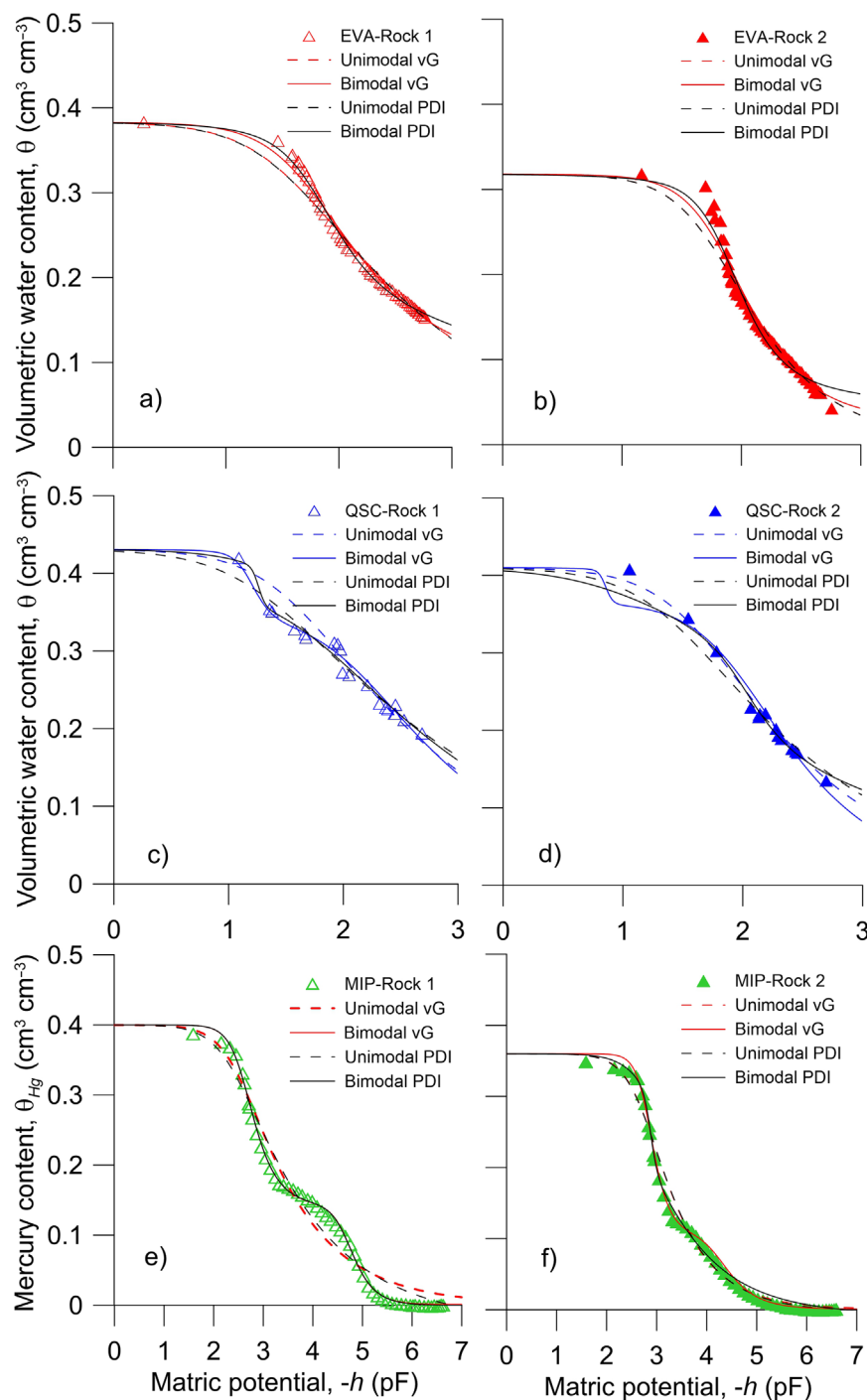
FIGURE 4 Water retention curves (WRCs) of Rock 1 and Rock 2 measured by evaporation (EVA) (a, b) and quasi-steady centrifuge (QSC) (c, d) methods; mercury retention curves (MRCs) of rocks (e, f). All the curves were fitted by the unimodal and bimodal van Genuchten (vG) and Peters Durner Iden (PDI) models. MIP, mercury intrusion porosimetry.

rocks. In addition, the QSC method has higher accuracy than other unsteady methods of comparable practicality, as stated in Caputo and Nimmo (2005).

The $K(h)$ data points measured by QSC for rocks (Figure 3c) seem to be generally consistent with those obtained by the EVA and DMSTF methods. Moreover, the $K(h)$ curves, obtained by QSC, cover four orders of magnitude of K, different from those measured by EVA and DMSTF methods that cover three and two orders of magnitude, respectively.

Except for the data of MRCs inferred by the MIP method, the retention and hydraulic conductivity functions were fitted simultaneously. The fitting of the data obtained with the EVA, QSC, ST, PC, and DMSTF provided the same model parameters for the two hydraulic functions. The θ values of the fitting are plotted versus negative h values, expressed in terms of pF, in order to be consistent with the experimental data (Figures 4 and 5; Tables 5–10).

For each WRC fitting model, the τ, θ_s, and θ_r measured values were fixed. Specifically, θ_r equals 0.001 for both the tested
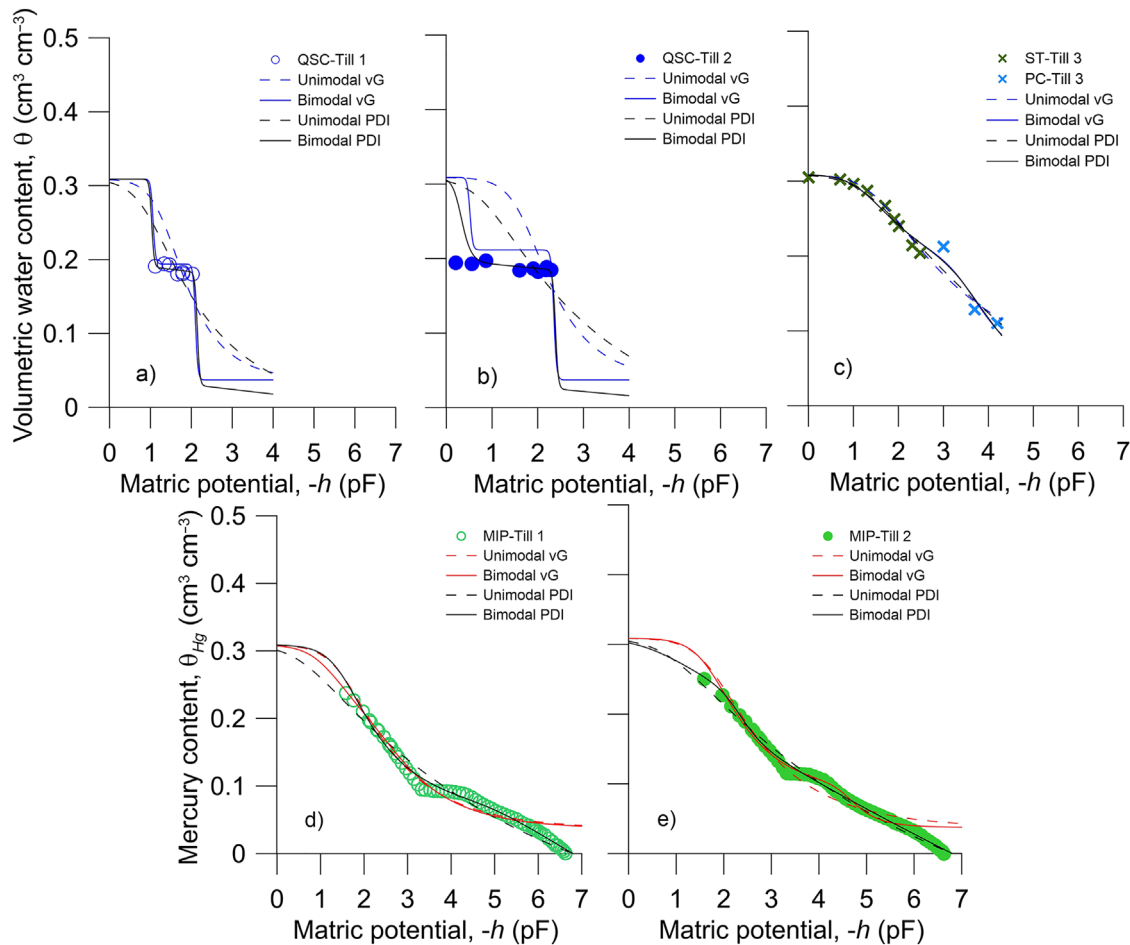
FIGURE 5 Water retention curves (WRCs) of Till 1 and Till 2 measured by quasi-steady centrifuge (QSC) (a, b) and of Till 3 measured by suction table (ST) (c) methods; mercury retention curves (MRCs) of Till 1 and Till 2 (d, e). All the curves were fitted by the unimodal and bimodal van Genuchten (vG) and Peters Durner Iden (PDI) models. MIP, mercury intrusion porosimetry; PC, pressure chambers.

rocks (Tables 5 and 6), while θ_s corresponds to the highest water content measured by each of the methods applied to the tested samples (Table 3; Figure 4a–d). For Rock 1, τ was fixed equal to 1.52 (Table 2), and the θ_s values were equal to 0.383 cm^3 cm^{-3} or 0.431 cm^3 cm^{-3}, corresponding to the highest water content obtained by EVA and QSC methods, respectively (Tables 5 and 6). For Rock 2, τ equals 1.56 (Table 2), and θ_s equals 0.318 cm^3 cm^{-3} or 0.41 cm^3 cm^{-3} depending on whether it was obtained by the EVA (Table 5) or QSC method (Table 6). The MRCs of rocks (Figure 4e,f) are better fitted by PDI models, both unimodal and bimodal one, showing the RMSE$_\theta$ values between 0.0047 and 0.0071, and AICc values between −577 and −534 (Table 7). Regarding the soils (Figure 5), the values fixed for the fitting were $\tau = 1.74$, while for θ_s and θ_r the values reported in Rieckh et al. (2012) were used corresponding to 0.309 cm^3 cm^{-3} and 0.037 cm^3 cm^{-3}, respectively. The higher θ_r value for soils compared to rocks is due to the clay content of the tested soils. The statistical analysis in terms of RMSE$_\theta$ as well as the AICc values, both considered to compare the performance of the different fitted

models (Tables 8 and 9), highlighted the goodness of fitting for Till 1 and Till 2 with the bimodal PDI model compared to the bimodal vG one. Instead, for Till 3, the bimodal vG model works better than the PDI one. Overall, the WRCs of all samples fitted by bimodal models show very low RMSE$_\theta$ values, that range between 0.0041 and 0.041, and AICc values that range between −153 and −97.

Figure 5a,b show a gap of experimental points in the wet range, due to the collapse of larger pores during centrifuge runs. Because of this gap, nothing could be gained in terms of fitting. Therefore, for the case of soils, the comparison of fitted models cannot give useful answers to discuss. WRC for Till 3, instead (Figure 5c), approaches the saturation, but it does not cover the dry range. Only soil MRCs (Figure 5d,e) cover the whole moisture range including the dry range. They are well fitted by the bimodal PDI model; in fact, their RMSE$_\theta$ values range between 0.0042 and 0.0174, and the AICc ranges between −605 and −433 (Table 10).

For the fitting of the hydraulic conductivity data (Figure 6a–d), the following were fixed: $K_s = 519$ cm
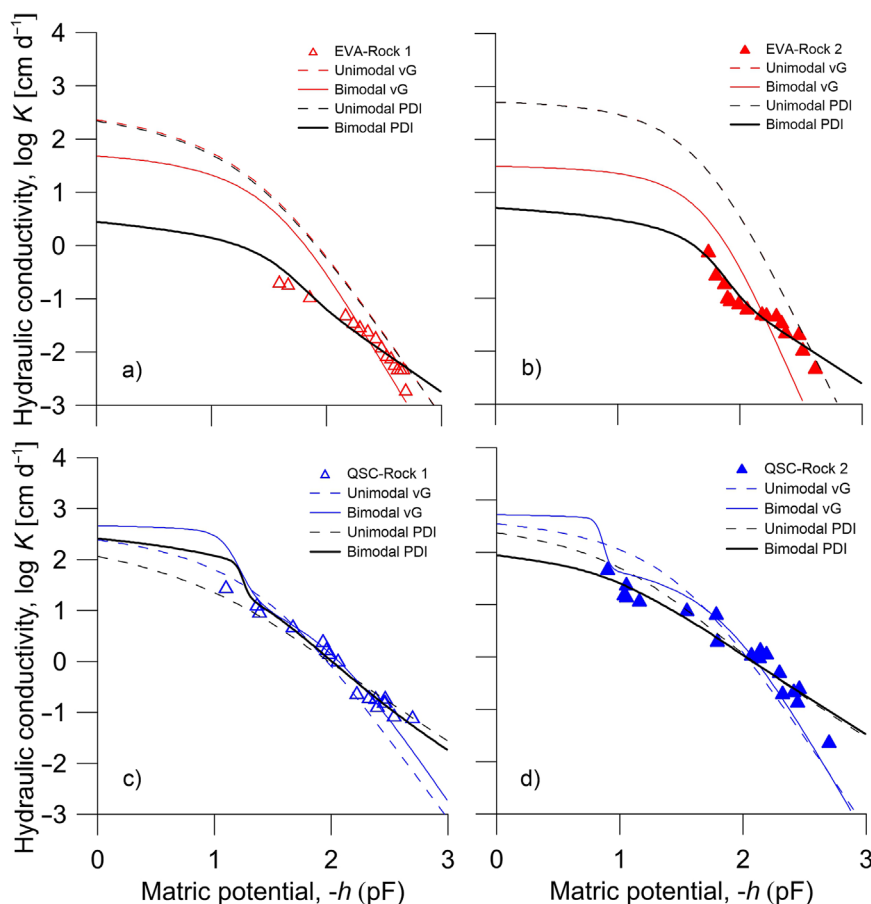
FIGURE 6 Hydraulic conductivity curves of rocks, measured by evaporation (EVA) (a, b) and quasi-steady centrifuge (QSC) (c, d) methods, fitted by the unimodal and bimodal van Genuchten (vG) and Peters Durner Iden (PDI) models.
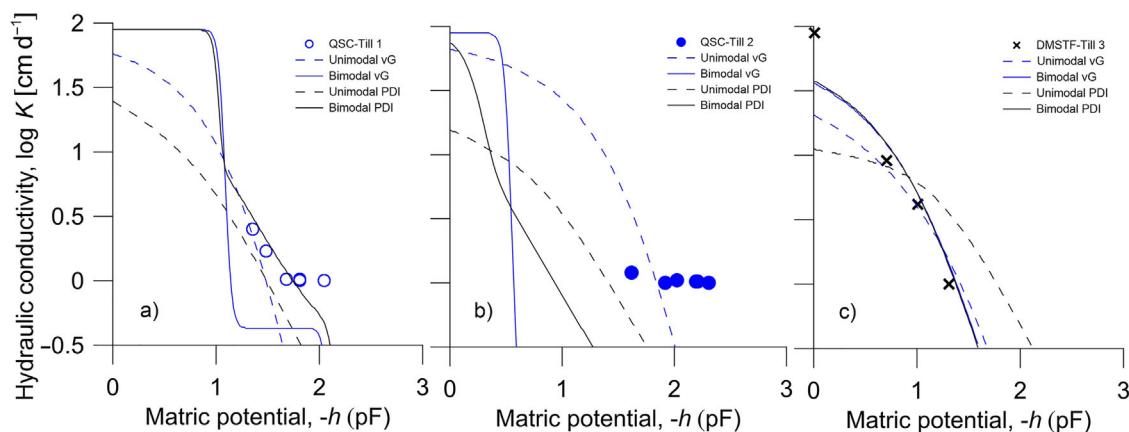

FIGURE 7 Hydraulic conductivity curves, of Till 1 and Till 2 measured by quasi-steady centrifuge (QSC) (a, b) and Till 3 by double-membrane steady-through flow (DMSTF) (c) methods, fitted by the unimodal and bimodal van Genuchten (vG) and Peters Durner Iden (PDI) models.

d^{-1} and $\tau = 1.52$ for Rock 1, $K_s = 555$ cm d^{-1} and $\tau = 1.56$ for Rock 2, and $K_s = 89.5$ cm d^{-1} (Rieckh et al., 2012) and $\tau = 1.74$ for the soils (Figure 7a–c).

The PDI bimodal model fitted the data better than unimodal ones (Figures 6 and 7) for all the samples, except for the $K(h)$ curve measured by QSC of Rock 1 and Till 2, where unimodal model fitted the data better (Tables 5, 6, 8,

and 9). The $K(h)$ curves of all samples show RMSE$_K$ values that range between 0.0041 and 1.2486, and AICc that ranges between −1003 and −97. Particularly, the bimodal PDI models exhibit lower RMSE$_K$ and higher AICc than the unimodal ones by corroborating the better quality of fitting using bimodal functions. For the same rock sample and for the same fitting model, the RMSE$_K$ obtained for data

FIGURE 8 Comparison between fitted curves by fixing (b, d) and not fixing (a, c) the tortuosity value for the water retention curves (WRCs) (above) and hydraulic conductivity (below). PDI, Peters Durner Iden; vG, van Genuchten.

4 | CONCLUSION
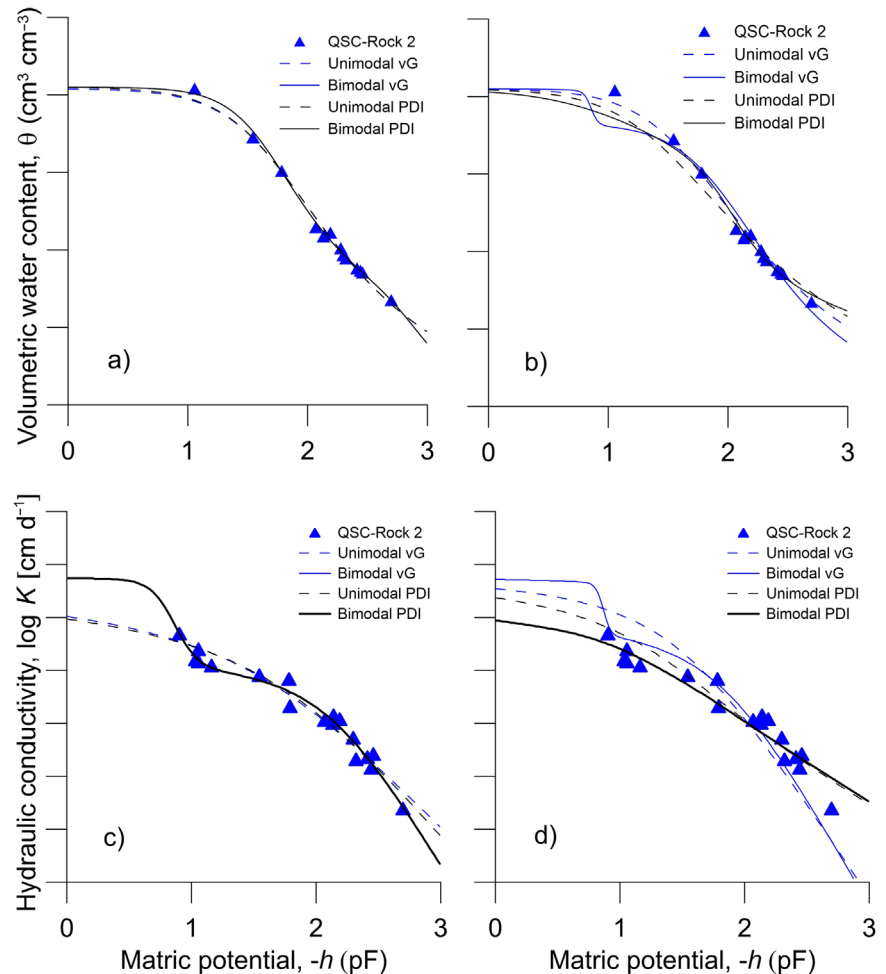
measured by QSC is lower than by EVA. This fact depends on the contrasting way of obtaining data between the two methods: the EVA method obtains experimental points by following the drying process, while the QSC method takes intermittent measurements during the forced draining of the sample. It is important to highlight that the fitting of the hydraulic conductivity data is worse compared to that of the retention data. This is attributable to the fact that the hydraulic conductivity is affected not only by pore size distribution but also by tortuosity of flow paths (Shinomiya et al., 2001; Zhong et al., 2016). In fact, for all the samples, the RMSE$_\theta$ value is low and ranges between 0.0041 and 0.0645, while the RMSE$_K$ shows higher values than RMSE$_\theta$, ranging from 0.1722 to 0.9783. This was because for the fitting, the measured value of tortuosity was used and not fitted. The differences between the fitted curves obtained by including the measured tortuosity value as compared to fitting the tortuosity value are limited to the near-saturated range of the hydraulic functions and especially affect the bimodal fits (Figure 8). Tables 5–10 display the parameters describing the goodness of fitting obtained by fixing or not the tortuosity parameter. They demonstrated that tortuosity affects the hydraulic conductivity curves, as expected, more than the retention curves.

The aim of this study was to re-evaluate the centrifuge approach in comparison with other laboratory methods for directly measuring the unsaturated hydraulic properties of porous carbonate rock and glacial till soil samples. For all the tested media, the water retention and unsaturated hydraulic conductivity functions were fitted by combining data obtained with the EVA, QSC, and DMSTF methods. The main novelties of this study lie in the direct determination of unsaturated hydraulic conductivity for rock and soil sample, the comparison among the investigated media, and the discussion of differences and similarities among the used methods. The results demonstrated that the QSC method, in contrast to both the EVA and the DMSTF methods, is capable of (i) more accurately capturing the bimodality of the rigid pore systems, (ii) allowing direct and fast K measurements, especially in the dry range, (iii) covering several ranges in the order of magnitude of the matric potential (iv) measuring values close to saturation as with the DMSTF method, and (v) getting a saturated water content value that is equal to the porosity. Specifically for soil samples, the application of the QSC method is limited by the nonrigid

structural characteristic despite such a relatively high bulk density.

The combination of data obtained by EVA, QSC, ST, and PC methods provided data for fitting WRCs in separate water content ranges. The QSC method covers a broader water content range of the WRC including that close to pore water saturation. Thus, a bimodal behavior as observed in the MRCs obtained from MIP was identified only with the QSC method. The fitted bimodal hydraulic conductivity curves were confirmed by the MIP-measured bimodal pore size distribution. Also, for the water retention, bimodal model fits were better than the unimodal ones, as corroborated by the $RMSE_\theta$, $RMSE_K$, and AICc values.

Overall, the results confirmed the uniqueness of the QSC method for measuring the hydraulic functions, particularly the conductivity, in a wider range of matric potential value and its limitation for nonrigid samples, even for highly dense soils. Results may help to provide improved hydraulic properties for numerical modeling of flow and transport processes to solve engineering and environmental problems.

AUTHOR CONTRIBUTIONS

ACKNOWLEDGMENTS

CONFLICT OF INTEREST STATEMENT

The authors declare no conflicts of interest.

ORCID

Maria C. Caputo https://orcid.org/0000-0002-0006-7796
Lorenzo De Carlo https://orcid.org/0000-0002-4823-4768
Antonietta C. Turturro https://orcid.org/0000-0002-8851-6604
Horst H. Gerke https://orcid.org/0000-0002-6232-7688

REFERENCES

Abell, A. B., Willis, K. L., & Lange, D. A. (1999). Mercury intrusion porosimetry and image analysis of cement-based materials. *Journal of Colloid and Interface Science*, *211*, 39–44. https://doi.org/10.1006/jcis.1998.5986

Akaike, H. (1974). A new look at statistical model identification. *IEEE Transactions on Automatic Control*, *19*(6), 716–723. https://doi.org/10.1109/TAC.1974.1100705

Andriani, G. F., & Walsh, N. (2007). The effects of wetting and drying, and marine salt crystallization on calcarenite rocks used as building material in historic monuments. *Geological Society, Special Publications*, *271*, 179–188. https://doi.org/10.1144/GSL.SP.2007.271.01.18

Andriani, G. F., & Walsh, N. (2009). Rocky coast geomorphology and erosional processes: A case study along the Murgia coastline South of Bari, Apulia—SE Italy. *Geomorphology*, *87*(3), 224–238. https://doi.org/10.1016/j.geomorph.2006.03.033

Andriani, G. F., & Walsh, N. (2010). Petrophysical and mechanical properties of soft and porous building rocks used in Apulian monuments (south Italy). *Geological Society, Special Publications*, *333*, 129–141. https://doi.org/10.1144/SP333.13

Basile, A., Albrizio, R., Autovino, D., Bonfante, A., De Mascellis, R., Terribile, F., & Giorio, P. (2020). A modelling approach to discriminate contributions of soil hydrological properties and slope gradient to water stress in Mediterranean vineyards. *Agricultural Water Management*, *241*, 106338. https://doi.org/10.1016/j.agwat.2020.106338

Bouma, J., Belmans, C., Dekker, L. W., & Jeurissen, W. J. M. (1983). Assessing the suitability of soils with macropores for subsurface liquid waste disposal. *Journal of Environmental Quality*, *12*, 305–311. https://doi.org/10.2134/jeq1983.00472425001200030002x

Campbell, G. S., Smith, D. M., & Teare, B. L. (2007). Application of a dew point method to obtain the soil water characteristic. In T. Schanz (Ed.), *Experimental unsaturated soil mechanics* (pp. 71–77). Springer Proceedings in Physics.

Caputo, M. C., & De Carlo, L. (2011). Field measurement of hydraulic conductivity of rocks. In L. Elango (Ed.), *Hydraulic conductivity—Issues, determination and applications* (pp. 285–306). Intech.

Caputo, M. C., De Carlo, L., Masciale, R., Perkins, K. S., Turturro, A. C., & Nimmo, J. R. (2023). Detection and quantification of preferential flow using artificial rainfall with multiple experimental approaches. *Hydrogeology Journal*, *32*, 467–485. https://doi.org/10.1007/s10040-023-02733-3

Caputo, M. C., De Carlo, L., & Turturro, A. C. (2022). HYPROP-FIT to model rock water retention curves estimated by different methods. *Water*, *14*(21), 3443. https://doi.org/10.3390/w14213443

Caputo, M. C., & Nimmo, J. R. (2005). Quasi-steady centrifuge method of unsaturated hydraulic properties. *Water Resources Research*, *41*, 1–5. https://doi.org/10.1029/2005WR003957

Dane, J. H., & Hopmans, J. W. (2002). Pressure cell. In J. H. Dane & G. C. Topp (Eds.), Methods of soil analysis, Part 4, physical methods *(1692)*. Soil Science Society of America.

da Silva, M. T. Q. S., do Rocio Cardoso, M., Veronese, C. M. P., & Mazer, W. (2022). Tortuosity: A brief review. *Materials Today: Proceedings*, *58*, 1344–1349. https://doi.org/10.1016/j.matpr.2022.02.228

De Carlo, L., Farzamian, M., Turturro, A. C., & Caputo, M. C. (2023). Time-lapse ERT, moment analysis, and numerical modeling for estimating the hydraulic conductivity of unsaturated rock. *Water*, *15*(2), 332. https://doi.org/10.3390/w15020332

De Carlo, L., Perkins, K. S., & Caputo, M. C. (2021). Evidence of preferential flow activation in the vadose zone via geophysical monitoring. *Sensors*, *21*(4), 1358. https://doi.org/10.3390/s21041358

Dirksen, C. (1991). Unsaturated hydraulic conductivity. In K. A. Smith & C. E. Mullins (Eds.), *Soil analysis physical methods* (pp. 209–270). Marcel Dekker.

Doussan, C., & Ruy, S. (2009). Prediction of unsaturated soil hydraulic conductivity with electrical conductivity. *Water Resources Research*, *45*(10), W10408. https://doi.org/10.1029/2008WR007309

Durner, W., & Lipsius, K. (2005). Determining soil hydraulic properties. In M. G. Anderson & J. J. McDonnell (Eds.), *Encyclopedia of hydrological sciences* (pp. 1121–1144). John Wiley & Sons.

Durner, W., Priesack, E., Vogel, H. J., & Zurmuhl, T. (1999). Determination of parameters for flexible hydraulic functions by inverse modeling. In M. Th. van Genuchten et al. (Eds.), *Characterization and measurement of the hydraulic properties of unsaturated porous media* (pp. 817–829). University of California, Riverside.

Farzamian, M., Monteiro Santos, F. A., & Khalil, M. A. (2015). Estimation of unsaturated hydraulic parameters in sandstone using electrical resistivity tomography under a water injection test. *Journal of Applied Geophysics*, *121*, 71–83. https://doi.org/10.1016/j.jappgeo.2015.07.014

Fu, X., Shao, M., Lu, D., & Wang, H. (2011). Soil water characteristic curve measurement without bulk density changes and its implications in the estimation of soil hydraulic properties. *Geoderma*, *167–168*, 1–8. https://doi.org/10.1016/j.geoderma.2011.08.012

Fujimaki, H., & Inoue, M. (2003). A flux-controlled steady-state evaporation method for determining unsaturated hydraulic conductivity at low matric pressure head values. *Soil Science*, *168*(6), 385–395. http://doi.org/10.1097/01.ss.0000075284.87447.cf

Ghambarian, B., Lin, Q., & Pires, L. F. (2023). Scale dependence of tortuosity in soils under contrasting cultivation conditions. *Soil and Tillage Research*, *233*, 105788. https://doi.org/10.1016/j.still.2023.105788

Globus, A. M., & Gee, G. W. (1995). A method to estimate moisture diffusivity and hydraulic conductivity of moderately dry soil. *Soil Science Society of America Journal*, *59*, 684–689. https://doi.org/10.2136/sssaj1995.03615995005900030008x

Horn, R., Peng, X., Fleige, H., & Dörner, J. (2014). Pore rigidity in structured soils-only a theoretical boundary condition for hydraulic properties? *Soil Science and Plant Nutrition*, *60*, 3–14. https://doi.org/10.1080/00380768.2014.886159

Hudson, D. B., Wierenga, P. J., & Hills, R. G. (1996). Unsaturated hydraulic properties from upward flow into soil cores. *Soil Science Society of America Journal*, *60*, 388–396. https://doi.org/10.2136/sssaj1996.03615995006000020009x

Hurvich, C., & Tsai, C. (1989). Regression and time series model selection in small samples. *Biometrika*, *76*(2), 297–307. https://doi.org/10.1093/biomet/76.2.297

Iden, S., & Durner, W. (2014). Comment to "Simple consistent models for water retention and hydraulic conductivity in the complete moisture range" by A. Peters. *Water Resources Research*, *50*, 7530–7534. https://doi.org/10.1002/2014WR015937

Iden, S. C., & Durner, W. (2007). Free-form estimation of the unsaturated soil hydraulic properties by inverse modeling using global optimization. *Water Resources Research*, *43*(7), 1–12. https://doi.org/10.1029/2006WR005845

IUSS Working Group WRB. (2014). *World reference base for soil resources 2014: International soil classification system for naming soils and creating legends for soil maps* (World Soil Resource Report no. 106). FAO.

Khanzode, R. M., Vanapalli, S. K., & Fredlund, D. G. (2002). Measurement of soil-water characteristic curves for fine-grained soils using a small-scale centrifuge. *Canadian Geotechnical Journal*, *39*, 1209–1217. https://doi.org/10.1139/t02-060

Kutílek, M. (2004). Soil hydraulic properties as related to soil structure. *Soil and Tillage Research*, *79*, 175–184. https://doi.org/10.1016/j.still.2004.07.006

Lipovetsky, T., Zhuang, L., Teixeira, W. G., Boyd, A., Pontedeiro, E. M., Moriconi, L., Alves, J. L. D., Couto, P., & van Genuchten, M. Th. (2020). HYPROP measurements of the unsaturated hydraulic properties of a carbonate rock sample. *Journal of Hydrology*, *591*, 125706. https://doi.org/10.1016/j.jhydrol.2020.125706

Masciopinto, C., & Caputo, M. C. (2011). Modeling unsaturated–saturated flow and nickel transport in fractured rocks. *Vadose Zone Journal*, *10*(3), 1045–1057. https://doi.org/10.2136/vzj2010.0087

Musso, A., Lamorski, K., Sławiński, C., Geitner, C., Hunt, A., Greinwald, K., & Egli, M. (2019). Evolution of soil pores and their characteristics in a siliceous and calcareous proglacial area. *Catena*, *182*, 104154. https://doi.org/10.1016/j.catena.2019.104154

Nimmo, J. R., & Akstin, K. C. (1988). Hydraulic conductivity of a sandy soil at low water content after compaction by various methods. *Soil Science Society of America Journal*, *52*(2), 303–310. https://doi.org/10.2136/sssaj1988.03615995005200020001x

Omoregie, Z. S. (1988). Factors affecting the equivalency of different capillary pressure measurement techniques. *SPE Formation Evaluation*, *3*(1), 147–155. https://doi.org/10.2118/15384-PA

Perkins, K. S. (2011). Measurement and modeling of unsaturated hydraulic conductivity. In L. Elango (Ed.), *Hydraulic conductivity–issues, determination and applications* (pp. 419–434). Intech.

Pertassek, T., Peters, A., & Durner, W. (2015). *HYPROP-FIT software user's manual, V.3.0*. UMS Gmbh.

Peters, A. (2014). Reply to comment by S. Iden and W. Durner on Simple consistent models for water retention and hydraulic conductivity in the complete moisture range. *Water Resources Research*, *50*, 7535–7539. https://doi.org/10.1002/2014WR016107

Peters, A., & Durner, W. (2015). *SHYPFIT 2.0 user's manual* (Research Report). Institut für Ökologie, Technische Universität Berlin.

Priesack, E., & Durner, W. (2006). Closed-form expression for the multi-modal unsaturated conductivity function. *Vadose Zone Journal*, *5*, 121–124. https://doi.org/10.2136/vzj2005.0066

Puhlmann, H., & von Wilpert, K. (2012). Pedotransfer functions for water retention and unsaturated hydraulic conductivity of forest soils. *Journal of Plant Nutrition and Soil Science*, *175*, 221–235. https://doi.org/10.1002/jpln.201100139

Ravina, I., & Magier, J. (1984). Hydraulic conductivity and water retention of clay soils containing coarse fragments. *Soil Science Society*

of American Journal, *48*, 736–740. https://doi.org/10.2136/sssaj1984.03615995004800040008x

Richards, L. A. (1931). Capillary conduction of liquids in porous mediums. *Physics*, *1*, 318–333. https://doi.org/10.1063/1.1745010

Rieckh, H., Gerke, H. H., & Sommer, M. (2012). Hydraulic properties of characteristic horizons depending on relief position and structure in a hummocky glacial soil landscape. *Soil and Tillage Research*, *125*, 123–131. https://doi.org/10.1016/j.still.2012.07.004

Romano, N., Hopmans, J. W., & Dane, J. H. (2002). Suction table. In J. H. Dane & G. C. Topp (Eds.), *Methods of soil analysis, part 4, physical methods* (pp. 692–698). Soil Science Society of America.

Schlüter, S., Leuther, F., Vogler, S., & Vogel, H. J. (2016). X-ray microtomography analysis of soil structure deformation caused by centrifugation. *Solid Earth*, *7*, 129–140. https://doi.org/10.5194/se-7-129-2016

Shinomiya, Y., Takahashi, K., Kobiyama, M., & Kubota, J. (2001). Evaluation of the tortuosity parameter for forest soils to predict unsaturated hydraulic conductivity. *Journal of Forest Research*, *6*, 221–225. https://doi.org/10.1007/BF02767097

Šimůnek, J., van Genuchten, M. Th., & Šejna, M. (2016). Recent developments and applications of the HYDRUS computer software packages. *Vadose Zone Journal*, *15*(7), 1–25. https://doi.org/10.2136/vzj2016.04.0033

Šimůnek, J., Wendroth, O., & van Genuchten, M. Th. (1999). Estimating unsaturated soil hydraulic properties from laboratory tension disc infiltrometer experiments. *Water Resources Research*, *35*, 2965–2979. https://doi.org/10.1029/1999WR900179

Singh, A., Haghverdi, A., Öztürk, H. S., & Durner, W. (2021). Developing pseudo continuous pedotransfer functions for international soils measured with the evaporation method and the HYPROP System: II. The soil hydraulic conductivity curve. *Water*, *13*(6), 878. https://doi.org/10.3390/w13060878

Sun, W. J., & Cui, Y. J. (2020). Determining the soil-water retention curve using mercury intrusion porosimetry test in consideration of soil volume change. *Journal of Rock Mechanics and Geotechnical Engineering*, *12*(5), 1070–1079. https://doi.org/10.1016/j.jrmge.2019.12.022

Turturro, A. C., Caputo, M. C., & Gerke, H. H. (2021). Mercury intrusion porosimetry and centrifuge methods for extendend-range retention curves of soil and porous rock samples. *Vadose Zone Journal*, *21*(1), e20176. https://doi.org/10.1002/vzj2.20176

Turturro, A. C., Caputo, M. C., Perkins, K. S., & Nimmo, J. R. (2020). Does the Darcy–Buckingham law apply to flow through unsaturated porous rock? *Water*, *12*, 2668. https://doi.org/10.3390/w12102668

van Dam, J. C., Stricker, J. N. M., & Droogers, P. (1990). From onestep to multi-step: Determination of soil hydraulic functions by outflow experiments (Report no. 7). Agricultural University.

van den Berg, E. H., Perfect, E., Tu, C., Knappett, P. S. K., Leao, T. P., & Donat, R. W. (2009). Unsaturated hydraulic conductivity measurements with centrifuges: A review. *Vadose Zone Journal*, *8*(3), 531–547. https://doi.org/10.2136/vzj2008.0119

van Genuchten, M. Th. (1980). A closed-form equation for predicting the hydraulic conductivity of unsaturated soils. *Soil Science Society of America Journal*, *44*, 892–898. https://doi.org/10.2136/sssaj1980.03615995004400050002x

Vrugt, J. A., Stauffer, P. H., Wohling, T., Robinson, B. A., & Vesselinov, V. V. (2008). Inverse modeling of subsurface flow and transport properties: A review with new developments. *Vadose Zone Journal*, *7*, 843–864. https://doi.org/10.2136/vzj2007.0078

Washburn, E. (1921). The dynamics of capillary flow. *Physical Review*, *17*, 273–283. https://doi.org/10.1103/PhysRev.17.273

Watson, K. K. (1966). An instantaneous profile method for determining the hydraulic conductivity of unsaturated porous materials. *Water Resources Research*, *2*, 709–715. https://doi.org/10.1029/WR002i004p00709

Wendroth, O., & Šimůnek, J. (1999). Soil hydraulic properties determined from evaporation and tension infiltration experiments and their use for modeling field moisture status. In M. Th. van Genuchten et al. (Eds.), *Characterization and measurement of the hydraulic properties of unsaturated porous media* (pp. 737–748). University of California, Riverside.

Wind, G. P. (1968). Capillary conductivity data estimated by a simple method. In P. E. Rijtema & H. Wassink (Eds.), *Water in unsaturated zone: Proceedings of the Wageningen symposium* (pp. 19–23). International Association of Hydrological Sciences and UNESCO.

Wöhling, T., Vrugt, J. A., & Barkle, G. F. (2008). Comparison of three multiobjective optimization algorithms for inverse modeling of vadose zone hydraulic properties. *Soil Science Society of American Journal*, *72*(2), 305–319. https://doi.org/10.2136/sssaj2007.0176

Young, M. H., & Sisson, J. (2002). Tensiometry. In J. H. Dane & C. G. Topp (Eds.), *Methods of soil analysis. Part 4: Physical methods* (pp. 600–620). Soil Science Society of America.

Zhang, J., Sirieix, C., Genty, D., Salmon, F., Verdet, C., Mateo, S., Xu, S., Bujan, S., Devaux, L., & Larcanch´e, M. (2023). Imaging hydrological dynamics in karst unsaturated zones by time-lapse electrical resistivity tomography. *Science of the Total Environment*, *907*, 168037. https://doi.org/10.1016/j.scitotenv.2023.168037

Zhong, R., Xu, M., Netto, R. V., & Wille, K. (2016). Influence of pore tortuosity on hydraulic conductivity of pervious concrete: Characterization and modeling. *Constructions and Building Materials*, *125*, 1158–1168. https://doi.org/10.1016/j.conbuildmat.2016.08.060

Zhuang, L., Bezerra Coelho, C. R., Hassanizadeh, S. M., & van Genuchten, M. Th. (2017). Analysis of the hysteretic hydraulic properties of unsaturated soil. *Vadose Zone Journal*, *16*(5), 1–9. https://doi.org/10.2136/vzj2016.11.0115

Zou, Z. Y., Young, M. H., Li, Z., & Wierenga, P. J. (2001). Estimation of depth averaged unsaturated soil hydraulic properties from infiltration experiments. *Journal of Hydrology*, *242*, 26–42. https://doi.org/10.1016/S0022-1694(00)00385-1